Yale 耶鲁大学-南京信息工程大学大气环境中心

Yale-NUIST Center on Atmospheric Environment

EUROPE'S 2003 HEAT WAVE: A SATELLITE VIEW OF IMPACTS AND LAND–ATMOSPHERE FEEDBACKS

Yale-NUIST Center of Atmospheric Environment

Yale Univ. and Nanjing Univ. of Infor. Sci. & Tech.

www.yale.edu www.nuist.edu.cn

Deng Lichen

2013-08-09

Outline

1.Introduction

2.Datasets and Data processing

3. Data Analysis
   3.1 Impacts on the land surface: drought and prolonged heat
   3.2 Surface energy budget; sensible heat flux ;

4. Conclusions

1.Introduction

The European heat wave of the summer of 2003 was an extreme climatic anomaly: the mean summertime temperatures over much of western and central Europe exceeded the 1961–1990 mean by up to 5 standard deviations, and the summer might have been the warmest since 1540.

Excessive heat and/or lack of water resulted in lower yields of grains, vegetables, fruits, and wines by between 4.6 and 10.8%, with uninsured crop losses totaling about US$12.3 billion. In France alone, officials estimated that wheat and corn harvests decreased by 15 and 28%, respectively, with losses totaling between US$1.1 and $4.4 billion.

Yale 耶鲁大学-南京信息工程大学大气环境中心

Yale-NUIST Center on Atmospheric Environment

2.Datasets and Data processing

2.1. Satellite imagery

Table I. Description of satellite data products and quality control preprocessing used in this study

Sensor	Product name	Product ID	Spatial resolution	Temporal resolution	Coverage dates	Product data layers utilized
MODIS Terra	Vegetative indices	mod13q1	250-m	16-day composite[d]	April–October (JD 97–288), 2000–2004	*NDVI*, Quality control (QC) flags[a]
MODIS Terra	Land surface temperature (LST) and thermal emissivity	mod11a2	1-km	8-day composite[d]	April–October (JD 97–288), 2000–2004	Day and night-time radiometric LST (approximately 10 a.m. and 10 p.m. overpass time), band 31 surface emissivity, QC flags
MODIS Terra	Bidirectional reflectance distribution function-corrected surface albedo	mod43b3	1-km	16-day composite[d]	April–October (JD 97–288), 2000–2004	Broadband white-sky albedo (bihemispherical reflectance) for the visible and near infrared[b]
MODIS Terra	Atmospherically corrected surface reflectances	mod09ghk	500-m	Daily	1 August 2000 and 10 August 2003	Band 1 and 2 (620–670 nm, 841–876 nm), QC flags
MODIS Terra	Land surface temperature (LST) and thermal emissivity	mod11a1	1-km	Daily	1 August 2000 and 10 August 2003	Day and night-time radiometric LST (approximately 10 a.m. and 10 p.m. overpass time), band 31 surface emissivity, QC flags
ASTER Terra	Atmospherically corrected surface reflectances	AST_03	15-m	Single day	1 August 2000 and 10 August 2003	Bands 1, 2, 3 (520–600 nm, 630–690 nm, 780–860 nm)
ASTER Terra	Atmospherically corrected surface albedo	AST_04	15-m	Single day	1 August 2000 and 10 August 2003	Broadband white-sky albedo (bihemispherical reflectance) for the visible and near infrared
ASTER Terra	Kinematic surface temperature	AST_07	90-m	Single day	1 August 2000 and 10 August 2003	1 temperature band[c]

[a] MODIS products are distributed with missing or corrupt data replaced with a null value. The present study used QC flags to identify potential snow and ice cover in the *NDVI* composites and to flag potential cloud-edge and thin cloud influence on reported land surface temperature. These data were eliminated from the calculations.

[b] White-sky albedo is calculated under the assumption of an isotropic diffuse radiation field and is equivalent to the hemispheric integral of direct albedo (Schaaf *et al.*, 2002).

[c] AST_07 product algorithms are described in Gillespie *et al.*, 1998.

[d] The MODIS compositing procedure is designed to minimize the influence that clouds and other atmospheric abnormalities have on the estimation of surface properties (Vermote and Vermeulen, 1999). The *NDVI* composite consists of the maximum daily *NDVI* value recorded with good quality at each pixel in the 16-day compositing period (Huete *et al.*, 1999). The land surface temperature composite uses an average of all clear-sky measurements obtained during the compositing period. The BRDF-corrected albedo composite takes advantage of multiple clear-sky looks to solve the bidirectional reflectance distribution function (Schaaf *et al.*, 2002).

2.2. Ancillary data

Daily records of precipitation, mean 2-m winds, and 2-m air temperature (mean, maximum, and minimum) from Climate Diagnostic Center archive of meteorological station records were used to construct an air temperature time series for all of France and to perform flux calculations at ASTER scale. A total of 126 stations in France reported a continuous data record between April 2000 and October 2004. Incoming radiation fluxes were obtained from the NCEP/NCAR reanalysis 6-hourly data archive ,as were winds and air temperature at $\sigma = 0.995$ (approximately 40 m height).

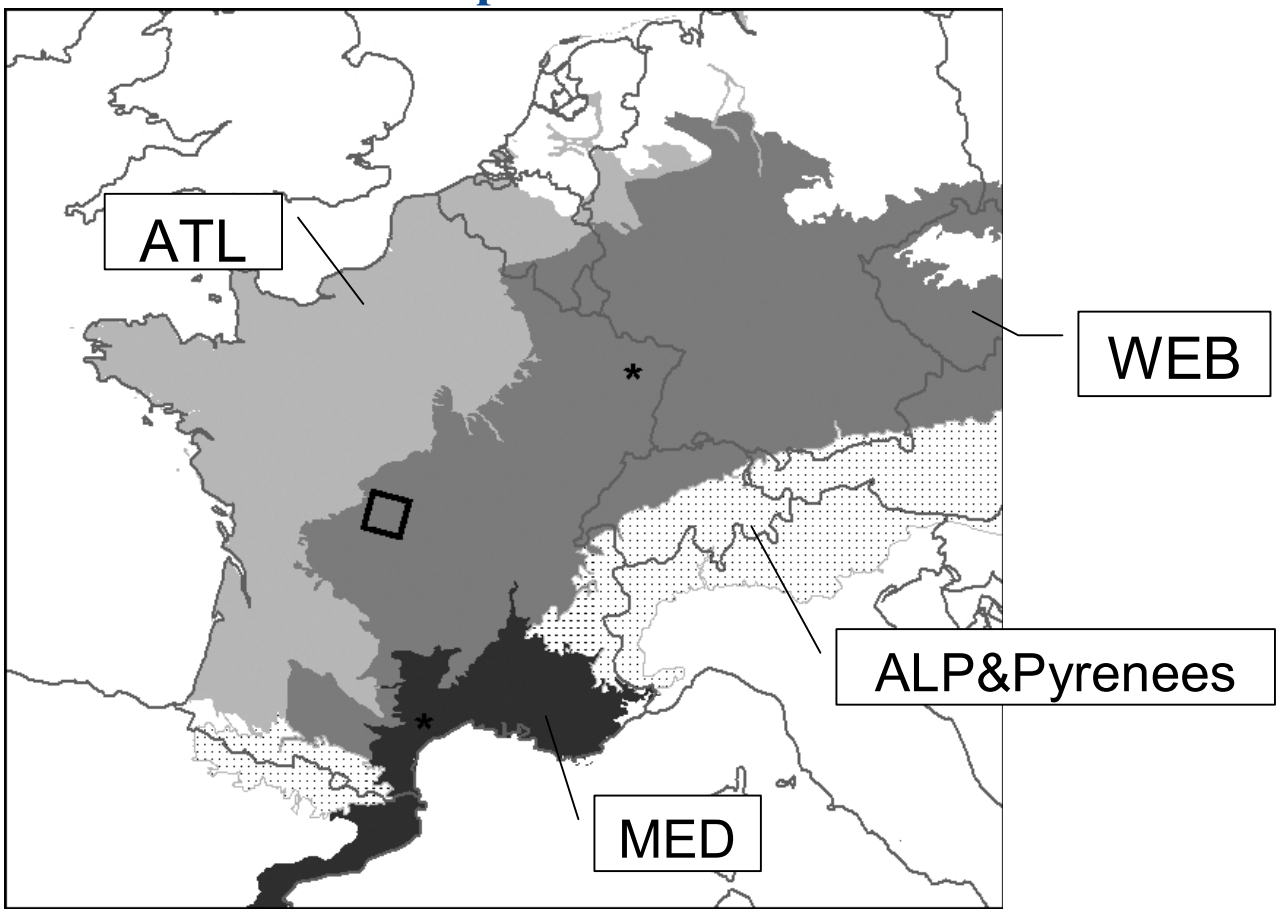

Figure 1. Dominant ecological zones of France – Mediterranean (dark gray) Western European Broadleaf Forests (medium gray), southern temperate Atlantic (light gray), and Alps and Pyrenees highland zones (striped). The black box shows the footprint of the ASTER image pair and stars are locations of Euroflux sites: Puechebon in the Mediterranean zone and Hesse Forest in the zone of western European Broadleaf Forests. Ecozone map European Environmental Agency, Copenhagen, 2000

Table II. Total area and average elevation of land-cover types within the three major ecozones and for all of France. Area is in km^2 and elevation is meters

Land cover	Mediterranean		W. Eur. Broadleaf		Temperate Atlantic		Alps		All of France	
	Area	Elevation	Area	Elevation	Area	Elevation	Area	Elevation	Area	Elevation
Crops	10 273	381	69 271	293	137 981	110	1 072	723	196 412	186
Pastures	1 280	633	45 060	447	32 911	116	985	1 001	70 663	327
Broadleaf and mixed forests	16 300	581	47 659	431	31 429	142	2 597	1 022	103 046	408
Coniferous forests	3 298	821	13 256	728	14 466	83	3 237	1 454	43 838	557
Orchards	8 019	122	1 479	258	4 396	76	46	355	11 729	124
Urban	1 461	163	6 062	294	11 503	73	398	683	24 613	164
Other	16 776	646	16 003	544	16 790	111	9 399	2 075	87 306	740
All	57 408	504	198 790	410	249 475	111	17 733	1 630	537 606	365

3.1.Impacts on the land surface: drought and prolonged heat

3.1.1 Vegetation

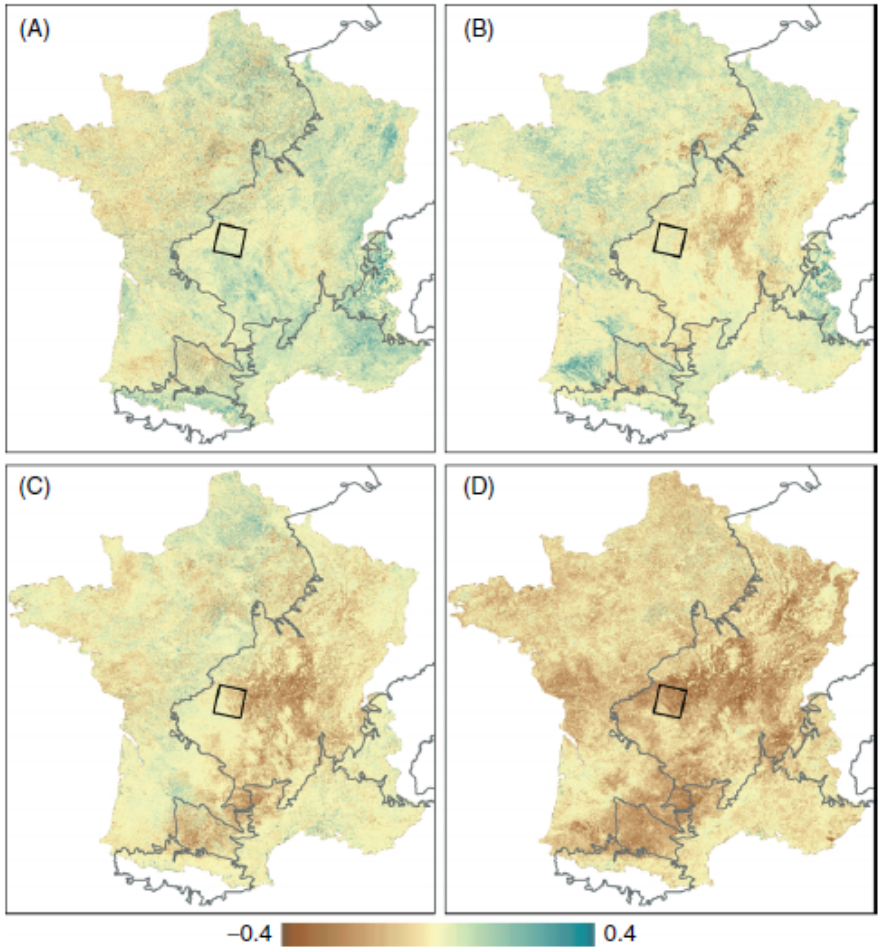

Figure 2. 2003 *NDVI* anomaly (*NDVI'*, unitless) calculated from MODIS 16-day composites for (A) 23 April–8 May, (B) 10–25 June, (C) 12–27 July and (D) 13–28 August. Ecological zones are outlined in gray; the ASTER footprint is indicated by the black box

3.1.1 Vegetation

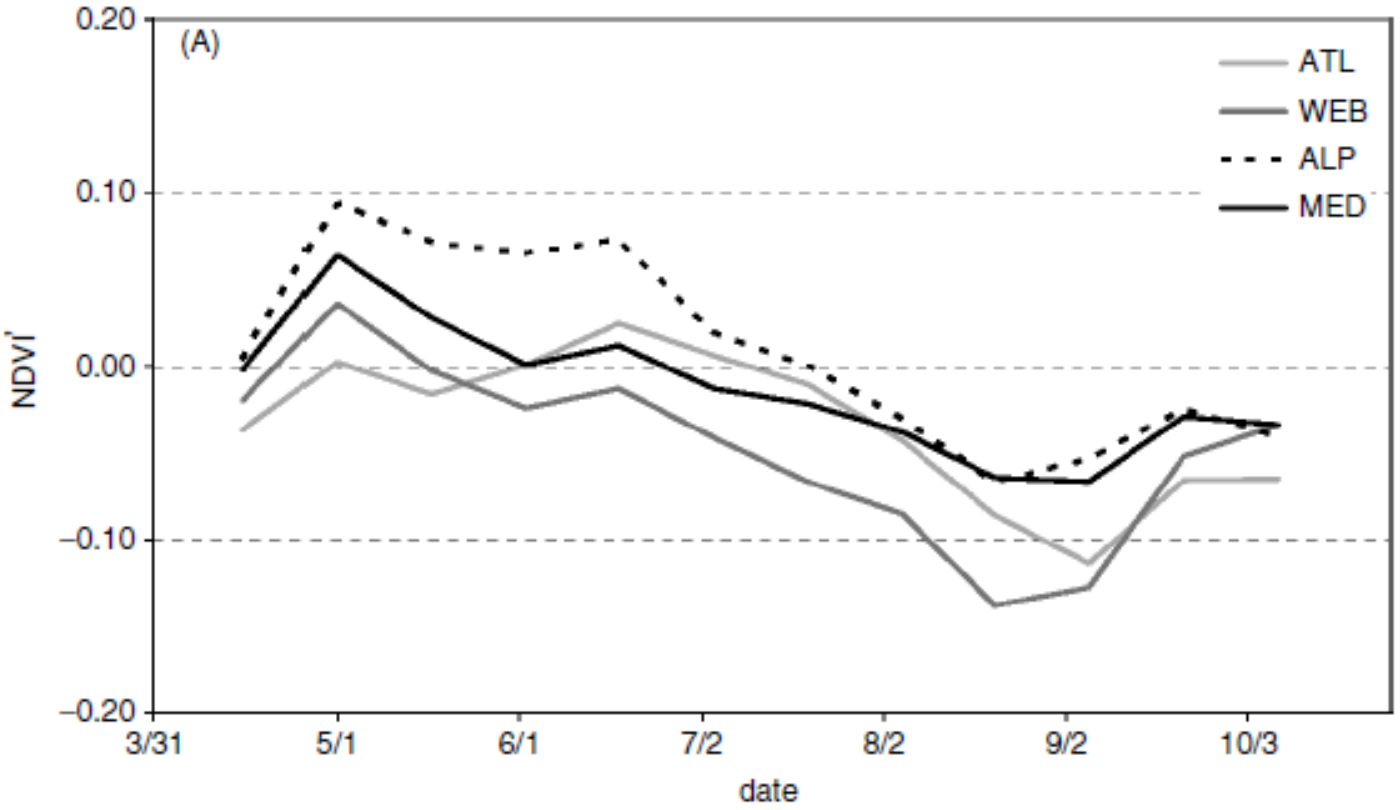

Figure 3. The 2003 anomaly in 16-day MODIS *NDVI* (*NDVI'*), averaged for each ecological zone. Time series of *NDVI'* calculated from all pixels, plotted at the mid-date of each composite period.

3.1.1 Vegetation

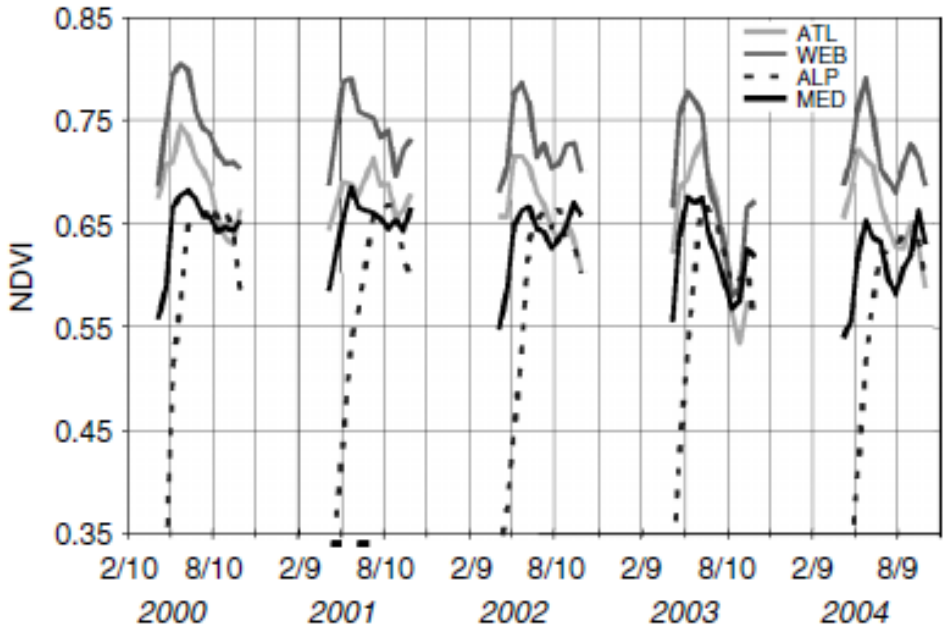

Figure 4. Spring and summer MODIS *NDVI* time series by ecological zone in France, 2000–2004. Data plotted at *NDVI* composite mid-date. Interpolations between missing/corrupted data points in May and July, 2001 are marked by bars along the *x*-axis

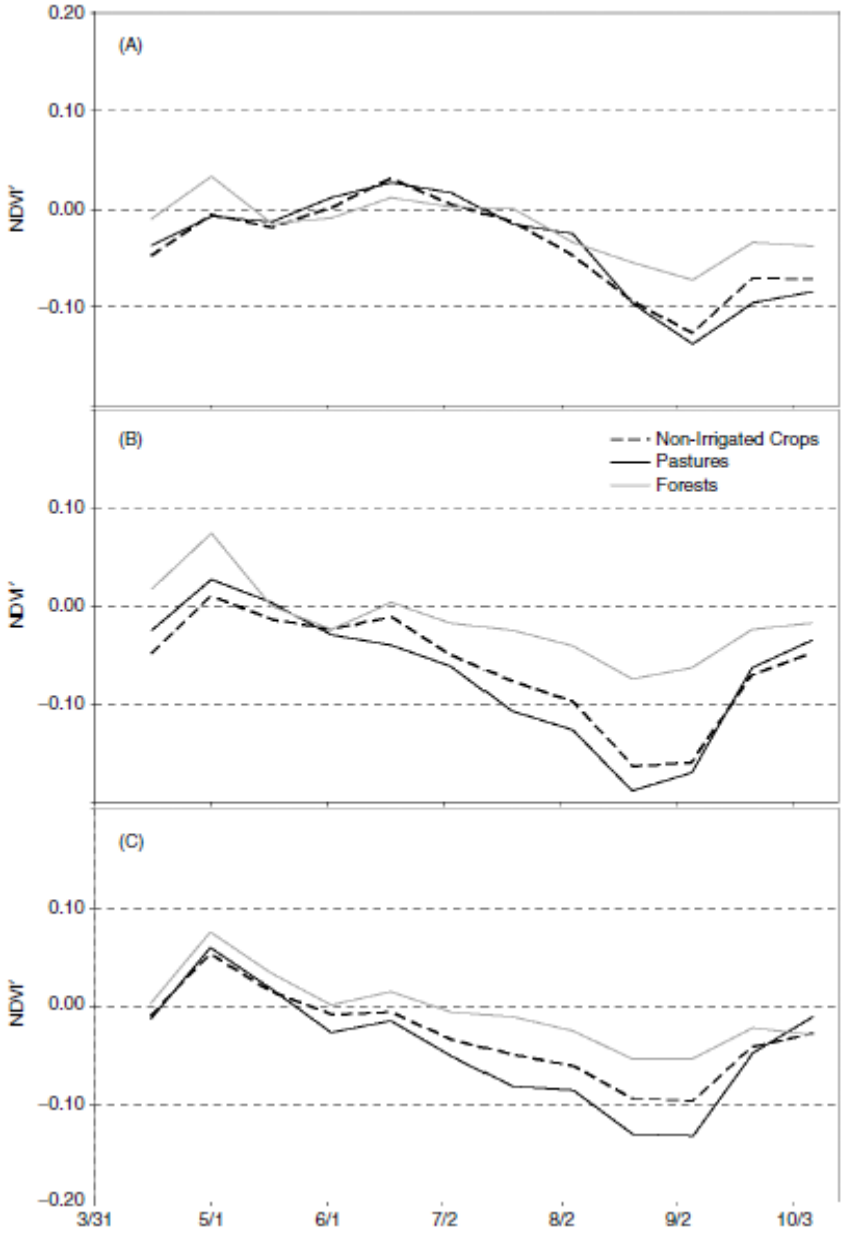

3.1.1 Vegetation

Figure 5. The 2003 MODIS *NDVI* anomaly (*NDVI* ') time series for dominant land-cover types in (A) ATL, (B) WEB, and (C) MED

3.1.2 Surface temperature

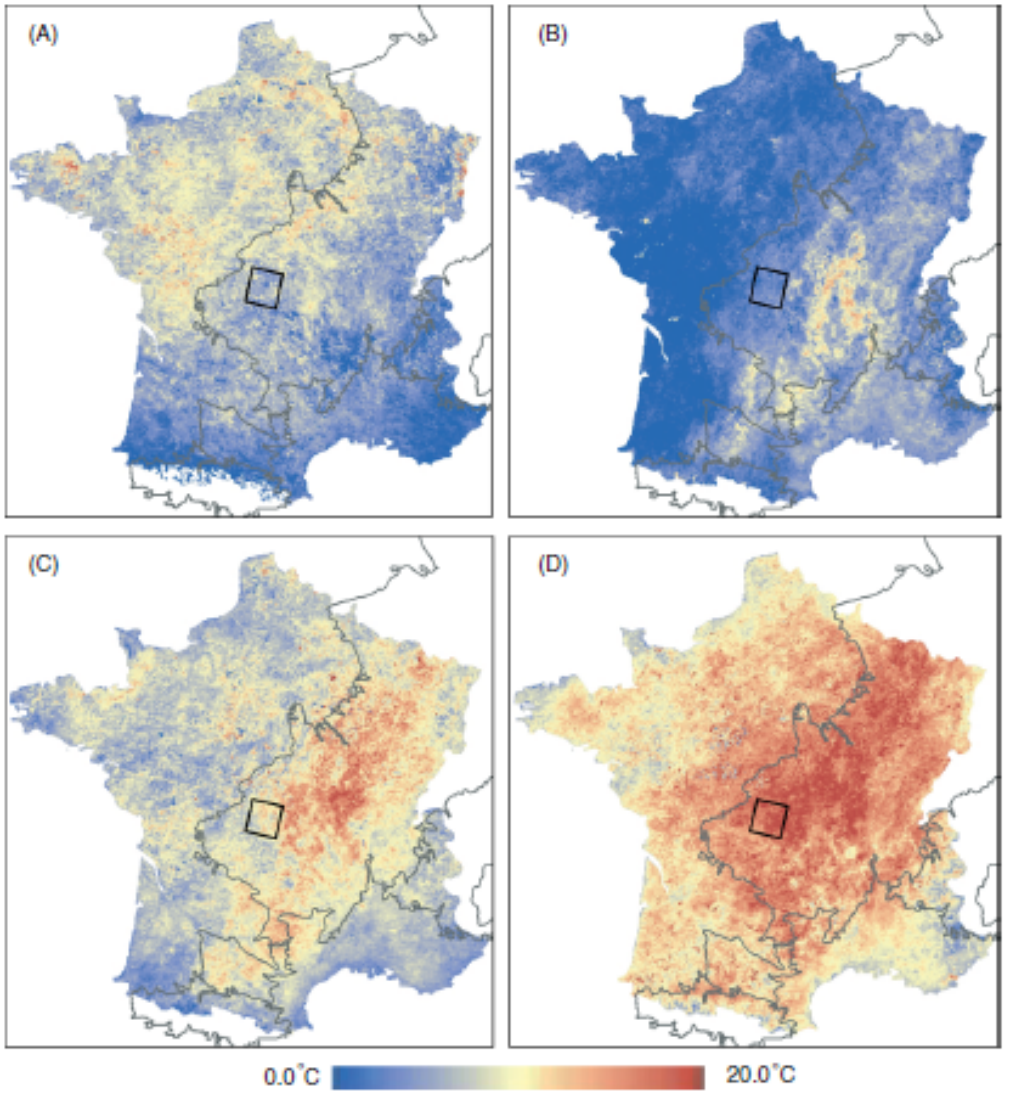

Figure 6. Spatial evolution of the 2003 radiometric temperature anomaly based on 8-day MODIS composites for (A) 15–22 April (B) 10–17 June (C) 12–19 July (D) 5–12 August. Ecological zones are outlined in gray; the ASTER footprint is indicated by the black box

3.1.2 Surface temperature

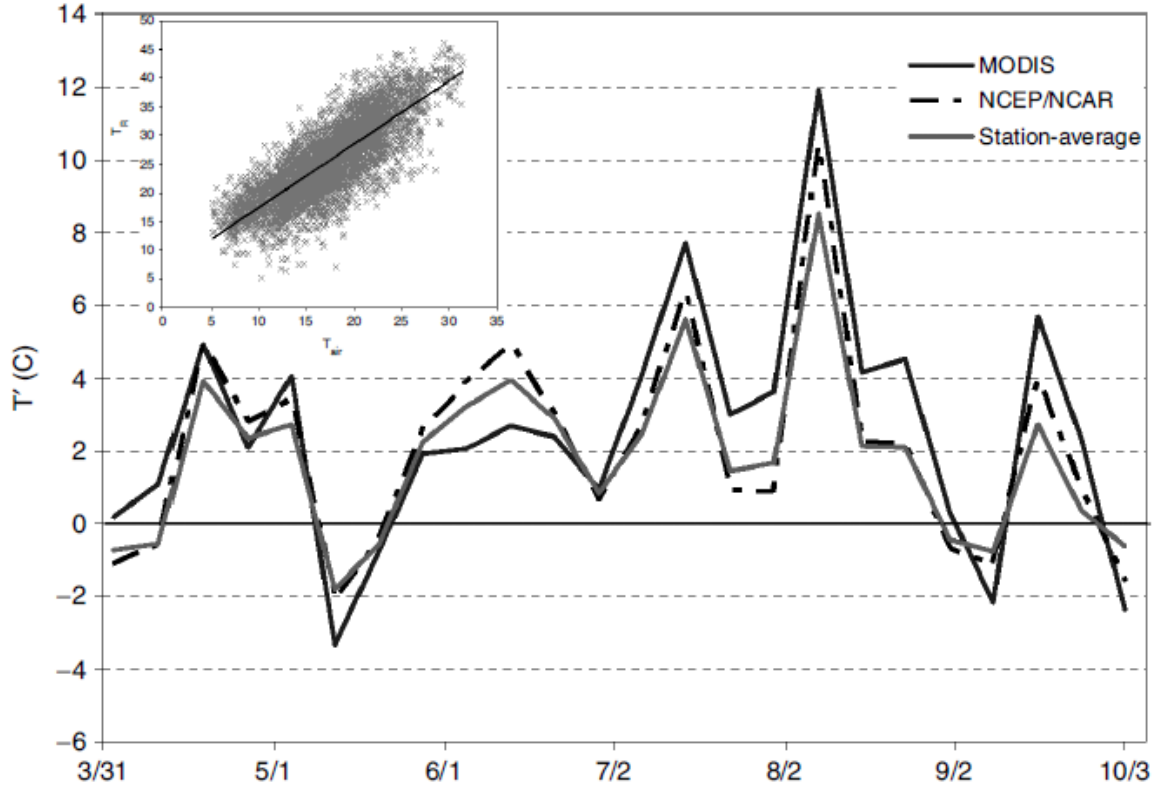

Figure 7. The 2003 temperature anomaly, plotted as 8-day averages for all of France from MODIS (T_R), from the NCEP/NCAR reanalysis ($T_{air}\sigma = 0.995$) and from the average of 126 meteorological stations (T_{air} at 2 m). Inset: Regression of 8-day average 2-m temperature *versus* MODIS 8-day radiometric surface temperature at the pixel containing the station. Data include all 8-day periods in 2000–2003 for which the mean temperature exceed 5 °C. The linear fit is $T_R = 1.105T_{air} + 6.4947$, $R^2 = 0.65$

3.1.2 Surface temperature

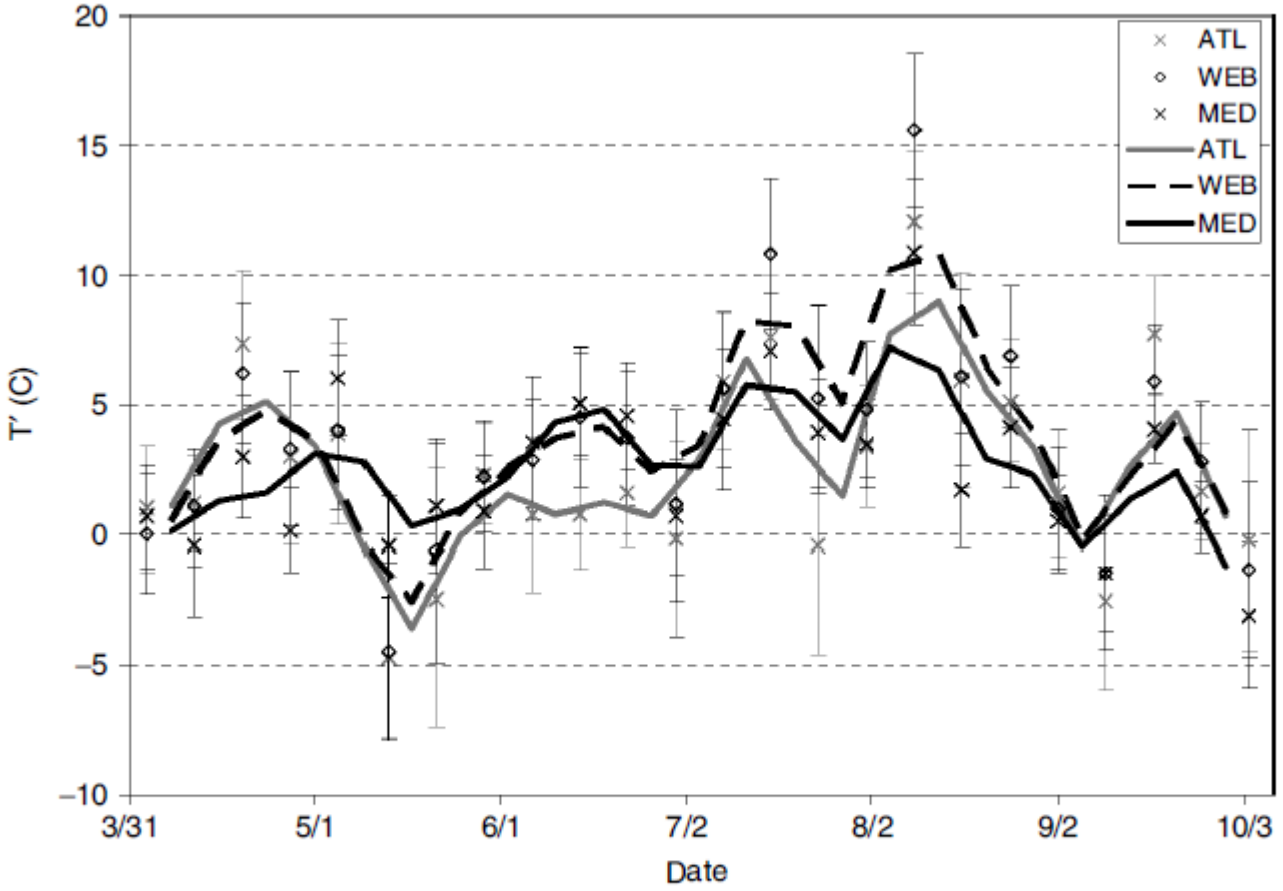

Figure 8. 2003 Radiometric temperature anomaly in each of the three dominant ecological zones. Points indicate the average value for each 8-day composite MODIS image in each ecological zone, error bars indicate ± one standard deviation within each ecological zone and lines are the 2-point running mean

3.1.2 Surface temperature

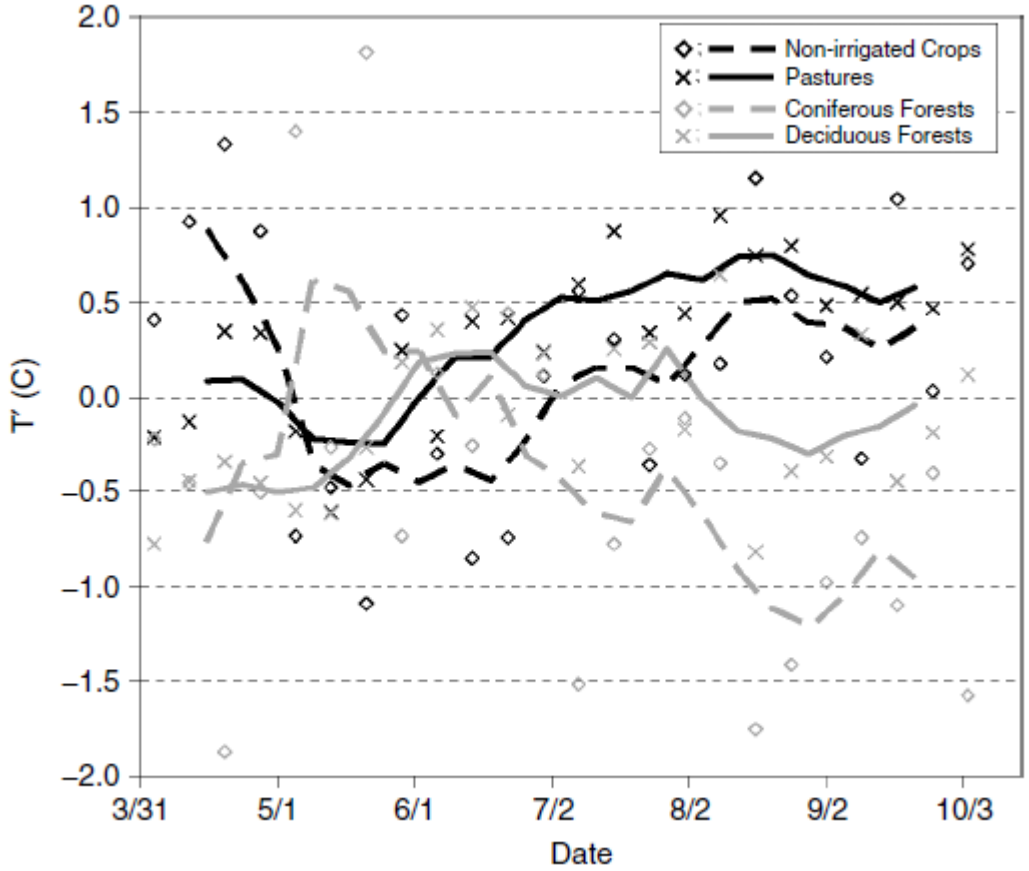

Figure 9. The influence of land cover on MODIS temperature anomaly. Points indicate the 2003 anomaly for each land use calculated relative to the mean 2003 anomaly for France at that date. Lines are the 4-point running mean for 8-day MODIS composite images

3.1.2 Surface temperature

It should be noted that T_R derived from MODIS composites represents an average for clear-sky days over the composite period; as clear days tend to be warmer than cloudy days, this may be an overestimate of the actual average T_R. According to the NECP/NCAR reanalysis, the summer of 2003 was considerably less cloudy than other years in the MODIS record for the study area. This suggests that the potential for warm bias in the composite-based T_R is less in 2003 than in other years, possibly introducing a conservative error to the calculation of radiometric temperature enhancement during the heat wave.

3.1.3 High-resolution analysis

2000-08-01 surface reflectance

2003-08-10 surface reflectance

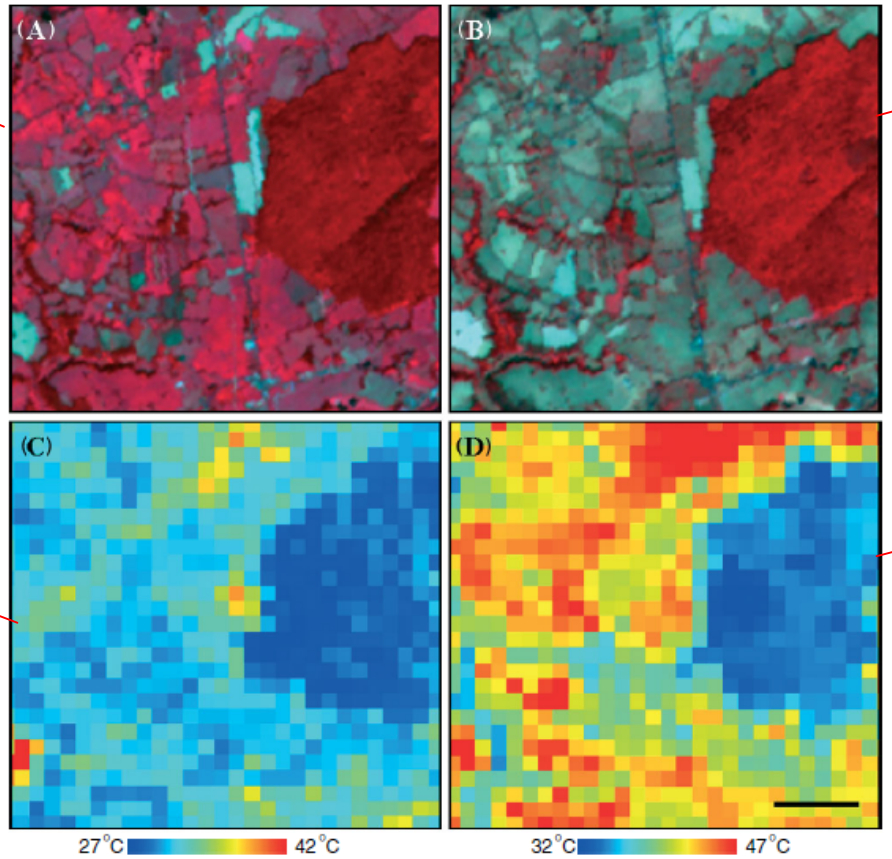

2000-08-01 surface temperature

2003-08-10 surface temperature

Figure 10. Level 2 ASTER products for a subset of the image footprint. (A), (B) Atmospherically corrected surface reflectances displayed as 321-RGB false color composites for the (A) 1 August, 2000 and (B) 10 August, 2003 images. Vegetation appears red because of the high reflectance in the near-IR (ASTER band 3). (C), (D) ASTER-derived kinematic surface temperature for the same (C) 2000 and (D) 2003 scenes. Note the large contrast between agricultural lands and forest patches in the 2003 image. Scale bar indicates 500 m and applies to all four images

Table III. Values of remotely sensed variables and air temperature for the ASTER image pair, 1 August 2000 and 10 August 2003. Bracketed values indicate MODIS averages over the area of the ASTER scene. MODIS *NDVI* and T_R are derived from single day images and MODIS albedo values are taken from 16-day white-sky albedo composites that include the dates of the ASTER images

Land Cover	Variable	2000	2003	Change
Scene average	T_{air} (C)	24	32	+8
	NDVI	0.73 [0.73]	0.55 [0.50]	−0.18 [−0.23]
	Albedo	0.21 [0.18]	0.20 [0.19]	−0.01 [+0.01]
	T_R (°C)	32 [31]	47 [44]	+15 [+13]
Forest	*NDVI*	0.87	0.87	0
	Albedo	0.19	0.17	−0.02
	T_R (°C)	29	40	+11
Villages	*NDVI*	0.45	0.46	+0.01
	Albedo	0.16	0.15	−0.01
	T_R (°C)	44	50	+6
Barren – barren cropland	*NDVI*	0.27	0.29	+0.02
	Albedo	0.24	0.22	−0.02
	T_R (°C)	47	58	+11
Active crops and pastures	*NDVI*	0.81	0.46	−0.35
	Albedo	0.21	0.22	+0.01
	T_R (°C)	31	51	+20
Active crops and pastures (no hedgerows)	*NDVI*	0.81	0.43	−0.37
	Albedo	0.22	0.22	0
	T_R (°C)	30	54	+24

3.2.1 Surface energy budget

The average white-sky surface albedo derived from MODIS was greatest for ATL throughout the period of analysis (0.18), intermediate in WEB (0.17), and lowest in MED (0.15). Neither the spatial pattern nor the absolute magnitude of albedo changed in 2003 relative to the MODIS era mean. This is somewhat surprising, given the expectation that drought will increase surface albedo ,but is consistent with some field studies and with the ASTER results in the present study.

In the ASTER analysis, the negligible change in broadband albedo can be explained in part by a decrease in near infrared reflectivity that offset the increase in reflectivity in the visible range.

3.2.2 Sensible heat flux

Averaged over the ASTER image, it estimates for instantaneous (10 a.m.) sensible heat flux are 227.7 (±119.3) W m^{-2} and 134.5 (±86.8) W m^{-2} for forests and the agricultural matrix (excluding bare soil), respectively, in 2000. The ± here represents the one standard deviation. The sensible heat flux for bare soil was not calculated because of the difficulty of estimating near-surface stability and temperature-correction terms. Variability within land-cover type is large relative to the difference between forests and agricultural lands, but the calculation indicates that the 2003 enhancement in sensible heat flux was greater for agricultural lands than for forests.

4. CONCLUSIONS

In summary ,the results of this study indicate that the heat wave of 2003 bore a phenomenological resemblance to model-predicted summers of the late twenty-first century .There was an unusually early spring green-up in response to the high temperatures in April. This was followed by a severe late-summer drought that was greatest in the ‘transitional belt’ between MED and ATL climate zones. The temperature anomaly was largest in south central France and was associated with substantially enhanced sensible heat flux.

If heat waves like that of 2003 become typical in the future European climate, then it is possible that ‘extreme’ events may change the observed trend in NDVI in some portions of Europe, with implications for regional hydrology, agricultural and forestry outlooks, and terrestrial carbon sequestration.

Thank you!